Low-temperature vibrational dynamics of fused silica and binary silicate glasses

Ling Cai, Ying Shi, Ken Hrdina, Lisa Moore, and Jingshi Wu
Science and Technology Division, Corning Incorporated, Corning, New York 14831, USA

Luke L. Daemen and Yongqiang Cheng
Chemical and Engineering Materials Division, Oak Ridge National Laboratory, Oak Ridge, Tennessee 37831, USA

(Received 27 August 2017; revised manuscript received 14 January 2018; published 21 February 2018)

Inelastic neutron scattering was used to study the vibrational dynamics of fused silica and its mixed binary glasses that were doped with either TiO_2 or K_2O. The energy transfer was measured from zero to 180 meV where the so-called Boson peaks (BP) at low energy and molecular vibrations at high energy are included. Although most of the vibrational spectra at the high energy resemble those reported in earlier literature, a defect-mode-like peak is observed for the doped binary systems near 120 meV. At very low temperature, the BP intensity increases rapidly with temperature and then, at higher temperature, the peak intensity decreases. As a result, a maximum is observed in the temperature dependence of the BP intensity. This maximum was shown in all four samples, but the pure SiO_2 sample shows the highest intensity peak and the lowest temperature for peak position. Broadband energy spectra reveal a shift of intensity from BP to the more localized modes at higher energy. Temperature evolution of BP and its relationship with heat conduction and thermal expansion are discussed.

DOI: 10.1103/PhysRevB.97.054311

I. INTRODUCTION

Low temperature thermodynamic property of glass is of great interest because of its close analogy to crystal systems in spite of their differences in structure. However in glasses, the appearance of excess density of states below 10 meV, which was coined Boson peak (BP) because of its phononlike behavior, seems to suggest that these anomalies are related to disorder in glass [1]. The peak appears on the plot of reduced density of state $g(E)/E^2$ vs E as excess of states, where according to Debye's theory $g(E)$ should be proportional to E^2. Earlier studies have attempted to explain the Boson peaks with phase transition either due to a saddle point in local potential landscape or jamming [2,3]. Evidences have also shown that, by scaling the peak intensity and energy, the Boson peaks are closely related to polymerization and annealing [4,5]. Recently, studies by Chumakov *et al.* showed that the Boson peaks are equivalent to the acoustic phonon in the crystalline phase counterpart, of which the difference is attributed to mass density [6–8]. While these interpretations have offered many hopeful insights into the nature of the Boson peaks, there still remains the unsolved mystery about its physical characteristics. One of the interesting behaviors of the Boson peaks is the temperature dependence. In many inelastic scattering experiments the Boson peaks are shown to decrease in intensity with increasing temperature [9,10]. The intensity change shows excellent correlation with other elastic properties such as sound velocity and modulus. However the temperature range of most of these studies are above the temperature at which the thermodynamic anomalies are observed [11].

Silicate glasses, including pure silica glass, are not only of great commercial value, but also present themselves as archetypical systems for many fundamental studies of glass phase transition, structural order, and vibrational dynamic properties. Even in its simplest form, namely fused silica, the structural correlations at different length scales are still not completely understood. Diffraction studies at very low momentum transfer have shown structural peaks that suggest intermediate range order or even porous structure below the first sharp diffraction peak [12]. Other studies have shown that the ringlike structure can be formed by corner sharing oxygens for several tetrahedra [13]. With the addition of species such as alkali or metal oxide into the silicate network, the structural heterogeneity is further complicated by the formation of nonbridging oxygen bonds and/or the change of local coordination number. As a result, a small addition of dopant can significantly change the thermodynamic properties such as thermal expansion and heat conduction.

In this study, inelastic neutron scattering is used to investigate the vibrational dynamics of silicate glasses from 5 to 300 K. Vitreous silica glass and its binary-mix systems were chosen for this study. Two types of dopants are incorporated in the binary systems, K_2O and TiO_2, which represent network modifier and network former additions, respectively. The doping levels are chosen to be not too high (5−10 mol%) to avoid complete crystallization. Nevertheless physical property differences in mass density and thermal expansion can still be observed. The energy range of the spectrometer covered from the elastic line to 500 meV, but meaningful vibrational spectra are only shown below 200 meV. The broadband energy vibrational spectroscopy can be qualitatively divided into three regions based on the underlying dynamic mechanism: (1) At very high energy the spectrum dynamics are dominated by the molecular bond vibrations. (2) At the intermediate energy, the dynamics are mostly related to tetrahedral grouped modes (TGM). These modes have correlation length on the order of one or a few tetrahedra. Therefore their dynamic properties

TABLE I. Chemical composition of oxide dopants R_2O or XO_2, mass density, and coefficient of thermal expansion of the four samples at room temperature.

Sample	R_2O or XO_2	ρ (g/cm^3)	α (ppb/C)
FS	Pure SiO_2	2.202	520
Ti5	TiO_2(5.67 mol%)	2.199	38
Ti8	TiO_2(8.03 mol%)	2.198	−144
K5	K_2O(5 mol%)	2.245	4110

are affected by the intermediate range order in glass. (3) At the lowest energy, the spectrum feature is entirely dominated by the Boson peaks, where the spectral intensity describes long wavelength elastic wave propagation. *ab initio* calculations were performed on amorphous silica and crystalline quartz to help the interpretation of vibrational modes. In the following sections, inelastic scattering data and analysis are presented in the order of decreasing energy. The temperature evolution of the spectrum lineshape is discussed in relationship to heat conduction and thermal expansion.

II. EXPERIMENTAL SETUP

Four binary samples were prepared at Corning for inelastic neutron scattering experiments. Three of the samples, fused silica (FS), TiO_2(5.7 mol%)-SiO_2 (Ti5), and TiO_2(8 mol%)-SiO_2 (Ti8) were produced by flame hydrolysis. In this process glass soot particles are generated in the flame and then deposited on a planar surface to form a porous layer. Subsequently the substrate is sintered at high temperature to form a dense glass. See for instance Ref. [14] for a detailed explanation of the process. The K_2O(5 mol%)-SiO_2(K5) was produced by crucible melt. The glass cullet were melted in Pt/Rh crucibles at 1650 °C for six hours, and the melts were poured into cold water to cool, then the glass cullet were dried overnight to remove water. The four samples are shown in Table I with their nominal chemical compositions and two macroscopic properties: mass density and thermal expansion coefficient at room temperature, which are characterized by Archimedean and dilatometry methods, respectively, at Corning. Ti8 has a blue color and is translucent while the other three samples are colorless and optically transparent.

Inelastic neutron scattering (INS) spectra were measured at the VISION spectrometer at the Spallation Neutron Source (SNS) in Oak Ridge National Laboratory (ORNL). VISION is a high-throughput, wide-band, indirect-geometry instrument using a white incident neutron beam for INS measurements. Glass samples were cut into 5 mm thick plates and sandwiched between two aluminum plates that were used to cool and heat the samples. The majority of the INS data were collected from 5 to 300 K. Additional measurements were taken at higher temperature to verify the continuous spectral behavior. The empty sample holder was measured at each corresponding temperature and the aluminum background signal was removed from the total INS spectra. All measurements were performed on heating, and a minimum of one hour of counting time was given at each scan. The obtained neutron cross section was corrected for Bose factor. The resulting reduced intensities are used to represent the generalized density of states $G(Q,E)$. Note that the INS data were not corrected for Q integration of the inelastic intensity because the indirect geometry instrument has a $\hbar\omega$ dependent Q intensity (See Fig. S1 in the Supplemental Material [15]). The instrument also produces a sharp $\lambda/2$ peak near 12 meV due to insufficient downstream filtering. However these artifacts should not introduce ambiguities to the well known high energy features in silicate glasses, or the temperature evolution of the scattering intensity. Multiple scattering and multiphonon scattering were shown to be negligible for VISION instrument (see, e.g., Fig. S2 in the Supplemental Material [15] for explanation). The overall shape of the obtained intensity spectra is in very good agreement with previously studied SiO_2 systems [16–19].

III. RESULTS

The *ab initio* calculation of lattice dynamics for α quartz and amorphous silica were performed using density functional theory as implemented in the CASTEP code. Simulation of VISION vibrational spectrum of the two materials are shown in Fig. 1(a). The similarity between α quartz and amorphous silica is clearly shown in the figure. Three sharp peaks at ∼100 meV, ∼130 meV, and ∼145 meV in α quartz are also seen in amorphous silica, but with a much more broadened line shape. According to the simulation and previous studies [16,19–21] these modes correspond to the O-Si-O vibration of transverse and two longitudinal normal modes, respectively. The broadened line shape in amorphous silica indicates that the localized molecular vibrations are heavily damped at long wavelengths. At lower energy, more complicated modes appear in the spectrum. Below 60 meV, a large number of modes that are related to the "rocking" and "bending" of oxygen tetrahedra become indistinguishable between quartz and amorphous silica. In the low energy region, one remarkable difference between the two systems is the appearance of a sharp phonon peak in quartz at ∼10 meV, but a similar sharp peak at 5 meV in amorphous silica, which agrees with the experimentally measured Boson peak. Figures 1(b) and 1(c) show the inelastic neutron scattering data of the four samples at 5 K and 300 K, respectively. The entire spectrum are corrected for Bose factor. The three main O-Si-O vibration modes have very similar spectral shape for all four samples at both 5 K and 300 K. Following the red dashed lines in the figure, there is no significant peak shift between samples, or between temperatures at 5 and 300 K. The apparent broadening at high temperature in all three peaks are likely due to Debye-Waller factor as the spectra are measured at relatively high **Q**. Near 120 meV, notably, there is a small intensity that can be seen in all the binary-mix samples but is absent in the FS sample. Earlier Raman scattering studies of titania silicate glass have attributed it to the Ti^{4+} related vibration modes [22,23]. Here, the peak is observed in both TiO_2 and K_2O mixed silicate glass, indicating that this peak is possibly related to the Si-O-X or Si-O-R bond vibrations in a mixed silicate system, as similarly speculated in an earlier study on the sodium titania silicate system [24].

At the intermediate energy range, a broad peak is observed from ∼20 to 60 meV. Earlier inelastic neutron scattering studies and the simulation work in this study suggest that the vibrations in this energy range are associated with twisting

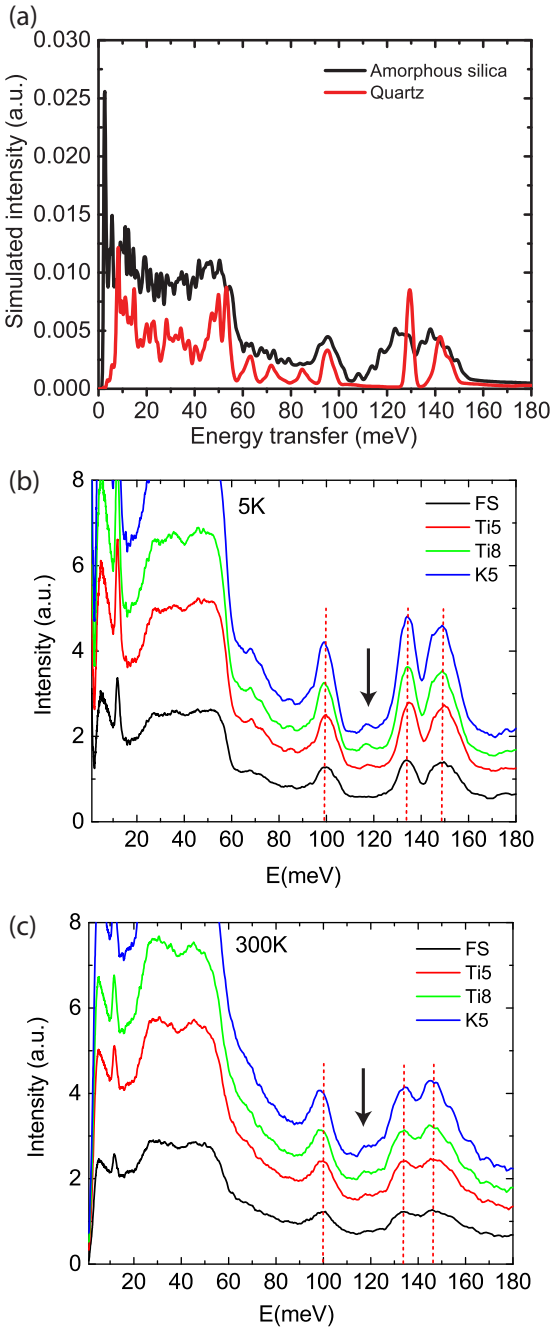

FIG. 1. Vibrational spectra from inelastic neutron scattering. (a) Simulated VISION spectrum for quartz and amorphous silica. Measured inelastic intensity and after correction for Bose factor for FS, Ti5, Ti8, and K5 samples are shown in (b) at 5 K and (c) at 300 K. The dashed lines are guides for the eye for the peak position. The arrows indicate the defect mode associated with the binary glasses. Constant offsets are given between measured intensities in (b) and (c) for clarity.

or rocking modes of neighboring tetrahedra [1]. Because of the large number of modes in the energy range, inelastic scattering data appears to be a broad peak [16,17,19,25]. The experimental data in this energy range do not show any discernible difference between the four samples.

Below the intermediate energy region, all glass systems show the pronounced Boson peaks. While the spectrum intensity in the high to intermediate energy range show very minimal differences for the four samples, their difference can be readily seen in the low energy range. The Boson peaks are shown as generalized reduced density of states $G(Q,E)/E^2$ in the inelastic neutron scattering data in Fig. 2, and it appears near 4 meV for all four glass samples. At high temperature, the intensity of these peaks decreases with temperature, while the peak position increases with temperature. However below 20 K, the intensity does not follow the same trend as the high temperature counterpart. In Fig. 2(e), the intensity of each sample at higher temperatures is normalized to their lowest temperature (5 K) intensity. It can be clearly seen that all samples exhibit an intensity maximum between 20 and 50 K, and the maximum in the FS sample at 20 K is the highest among the four. At higher temperatures, it is noted that among the three doped silicate samples the BP intensity diminishes the fastest in the Ti8 samples and the slowest for the K5 sample, while the Ti5 intensity decreases moderately between the Ti8 and K5 samples.

To further illustrate the temperature evolution of the intermediate to low energy spectrum intensity, the data are plotted as the difference in the intensity between higher temperatures and the lowest temperature (5 K) intensity, see Fig. 3. Each plot is schematically separated into lightly shaded "BP region" for BP dynamics and cross hatched "TGM region" for tetrahedral grouped motion dynamics in the intermediate energy range. In these plots, it is evident that the spectrum intensity shifts with temperature towards higher energy regions. The decrease in BP intensity above 50 K is accompanied by the increase of intensity in the TGM region. The position of the intensity-difference maximum approximately follows the thermal energy, k_BT. This is an indication that the dynamical mechanism in the intermediate to low energy region can be driven by thermal excitation. The exact maximum position would depend on the underlying vibrational dynamics in the specific energy range. But because of the high mode density in the intermediate energy range, the intensity maximum is seen to shift continuously with respect to temperature. The intensity shift is indiscriminate between the four glasses, which suggests that SiO_2 tetrahedral motions dominate the intermediate energy range. At the very low temperature ($<$20 K), the thermal energy is below the Boson peaks, therefore no intensity-difference maximum is observed in the entire energy range. Near 20 K the intensity difference shows a strong maximum in the BP region, which indicates a strong absorption of the thermal energy by the Boson peaks. At T $>$ 20 K, as the intensity-difference maximum shifts to the TGM region, spectral differences amongst the four samples are small. Nevertheless, a subtle difference for the K5 sample can be seen in the BP region of the spectrum where its intensity decrease is much less than the other three samples.

IV. DISCUSSION

For all four measured samples, the difference in the high energy inelastic spectrum is small. The predominant features for this energy range come from O-Si-O vibrations. However, Figs. 1(b) and 1(c) show that the three binary systems unequivocally exhibit a weak peak near 120 meV. This peak was previously reported from Raman scattering of titania silicate

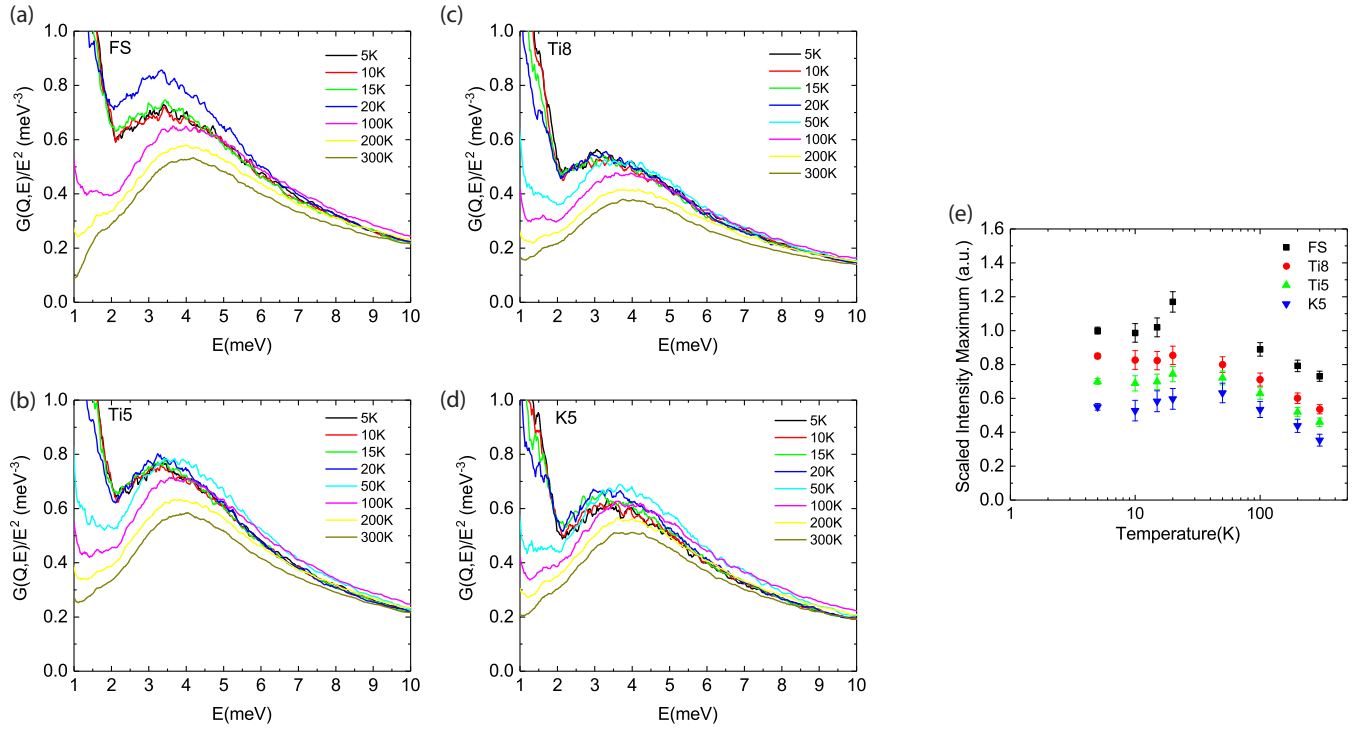

FIG. 2. Reduced density of states in the BP region from 5 K to 300 K for FS, Ti5, Ti8, and K5 are shown in (a), (b), (c), and (d), respectively. Scaled BP max intensity for each sample is shown in (e), see text for explanation.

glass [22], but could not be attributed to any structural mode of Ti local coordination. The fact that this peak is present in all doped samples but missing in the fused silica sample suggests that it is related to a O-Si-O vibration mode where the oxygen motion is strongly coupled to the nearest neighbor K or Ti. Note that K and Ti show substantial differences in local coordination in silicate glasses. Hence it is unlikely their intrinsic K-O or Ti-O vibration modes could appear at the same energy, e.g., 120 meV.

The broad peak from ∼20 to 60 meV is comprised of a large number of modes that describe tetrahedral grouped motions. Because of the high density of modes in this energy region, the instrumental resolution broadened spectra appear to be a broad peak. Although the correlated tetrahedral motion are generally regarded as harmonic in nature, their intensity, within the measurement temperature range, does shift with temperature. As temperature increases, the intensity near the ∼ 20 meV shoulder decreases while the intensity at the ∼60 meV shoulder increases. The continuous shift of intensity in the intermediate energy range indicates a relaxational nature of these vibrational modes.

Below the broad peak all four samples show the prominent Boson peaks near ∼4 meV. However, a remarkable difference is observed between fused silica and the other three binary samples below 50 K. The continuous increase of intensity between 5 and 20 K in fused silica suggest that the Boson peaks in this energy range are strongly coupled to thermal excitations. Nevertheless, in the doped samples the change in BP intensity is much slower. This is shown in Fig. 2(e) where the intensity of Ti8, Ti5, and K5 samples rise much less rapidly as compared to the FS sample. The slower increase suggests that the thermal excitation contributions to the Boson peaks are strongly damped by the presence of network impurities. However the distinctive roles of modifier and network former are not clear at the moment. It is interesting to point out that at very low temperature the density of states is closely related to other thermodynamics properties such has heat conduction. The phonon mean free path can become comparable or longer than the phonon correlation length at low temperature [26]. Hence the glass and crystal systems are often treated similarly as elastic continuum [27]. A strong scattering of the low frequency phonon is likely to reduce the heat conduction. A wide range of reports have shown that there exist a low-temperature plateau region for thermal conductivity in silicate glasses, and the anomaly is more pronounced in doped silicate glasses than in pure fused silica [28–30]. This plateau region coincides with the BP intensity maximum at ∼20 K. The excellent correlation between the two seems to suggest that the Boson peaks, as the lowest energy vibrational mode, interact strongly with heat-carrying phonons below 20 K, while a transition to a conduction by shorter range correlation occurs at >20 K, and eventually the conduction is dominated by the short range structural modes at higher energy. It is interesting to note that in the similar temperature region, vitreous silica has a maximum negative thermal expansion [31]. The decrease of intensity above 20 K was similarly reported in previous studies [9,32], and excellent correlation was observed between the intensity change and elastic properties. Here, it is evident from Fig. 3 that the decrease of BP intensity is accompanied by the increase of intensity in the broad peak in the intermediate energy range (TGM region). The continuous increase of spectrum intensity from the Boson peaks to ∼50 meV seems to suggest that, similar to heat conduction, the elastic properties are determined by the transfer of energy from the

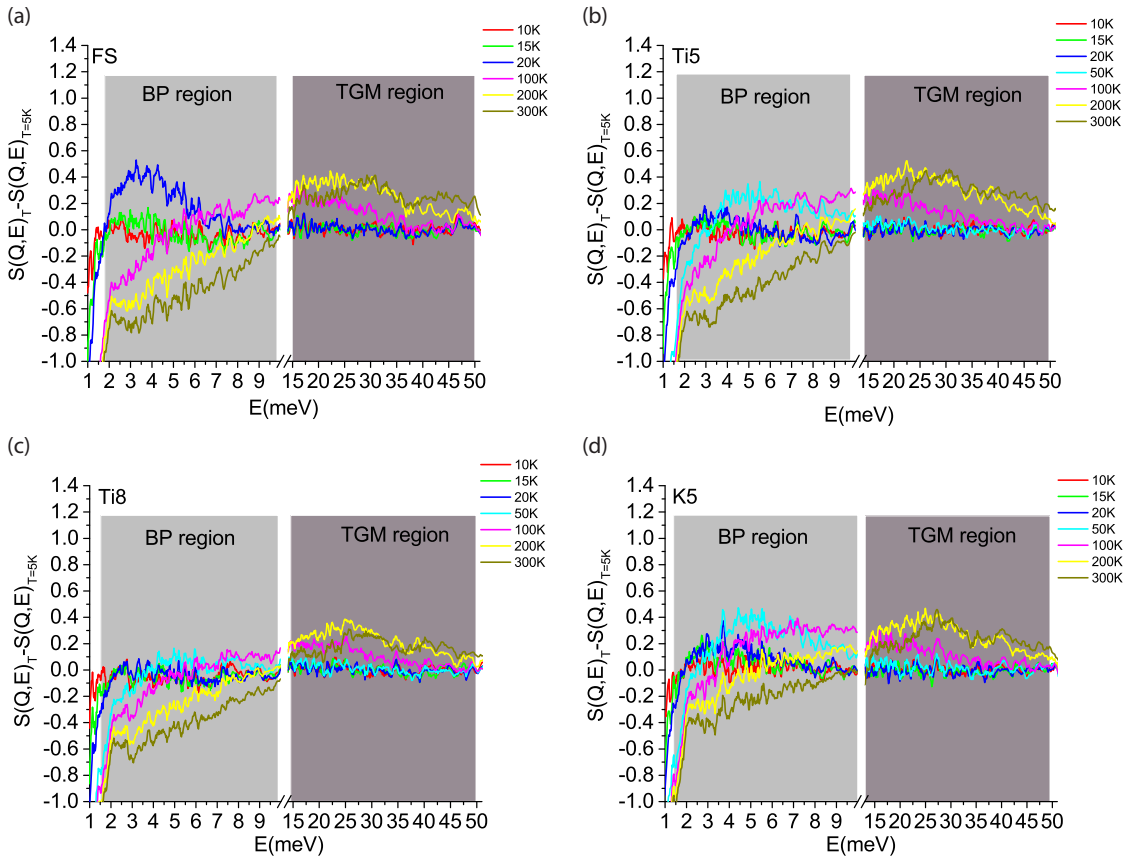

FIG. 3. The difference in intensity between high temperatures and the lowest temperature (5 K) are plotted in (a) through (d) for sample FS, Ti5, Ti8, and K5, respectively. The shaded colors in each plot conceptually separates the intensity into two dynamical regions based on spectral features.

acoustic phononlike dynamics to the more localized vibrational modes.

One interesting property that differentiates the four samples beside their chemical composition is the thermal expansion. In Table I, the listed coefficient of thermal expansion near room temperature shows orders of magnitude differences. K5 sample has the highest coefficient of thermal expansion that is a few parts per million while the other three samples are on the order of parts per billion [33,34]. The same studies showed that addition of titania reduces thermal expansion while the addition of potassium (and similar alkali species) increase the thermal expansion in extended temperature range. From the classical theory of quasiharmonic approximation, certain aspects of thermal expansion can be studied through the phonon density of state in the region where the phonon frequency is similar to the thermal energy of interested temperature range [35,36]. From 200 to 600 K, where the largest thermal expansion differences between the four samples were observed, the thermal energy resides between ∼17 and 50 meV. Our theoretical calculation and experimental data show that it is very difficult, at least for the technique used in this study, to resolve phonon modes in this energy range. As a result, we did not observe any pronounced shift of peak intensity corresponding to thermal expansion as reported in an earlier study of a negative thermal expansion system ZrW_2O_8 [36]. However one noticeable difference between the four samples at room temperature is the change of BP intensity as shown in Fig. 3. The figure revealed that the BP intensity change is much smaller in the K5 sample than that of the other three samples. The ability to retain long-range wave propagation in the K5 sample could suggest that the thermal expansion property in this material is less affected by anharmonic effects in localized vibrations than that of the other three samples. It is interesting to note that at the temperature where the maximum of Boson peak intensity is observed, a maximum of negative thermal expansion is also reported in silica glass [31]. It seems that this is a temperature region where many thermodynamic anomalies are observed, and one possible explanation is that at this temperature the glass system transitions from a classical description to a quantum mechanical model such as the one described very early by Anderson *et al.* [26].

V. CONCLUSION

The four silicate glass samples investigated in this study differ in their chemical compositions. Beside the fused silica sample, K or Ti was added to form binary silicate glasses in the other three samples. In the neutron experiment, very similar O-Si-O bond vibration modes were observed in all four samples at ∼100, 130, and 145 meV. Because of the relative constant lineshape of the three peaks with respect to samples and to temperatures, we conclude that these high

energy molecular vibrations have very minimal contribution to physical properties such as thermal expansion and heat conduction, which are very distinct among the four samples. The observation of the weak peak at 120 meV in the three binary samples seems to suggest this is a universal feature for dopant related defect mode in silicate glasses.

At lower energy, while the broad peak between 20 and 50 meV is indistinguishable between samples, the Boson peaks at 4 meV show discrepancy between fused silica and the binary systems. The intensity change in the Boson peaks suggests a strong correlation between the scattering effect of phononlike long-range wave propagation and the plateau of thermal conductivity at low temperature. Moreover the continuous shifting of intensity towards higher energy on increasing temperature indicates that tetrahedral grouped motions can effectively absorb thermal energy, and the vibrational modes in this energy range are coupled to relaxational mechanism. The temperature evolution of the spectrum intensities in the low-temperature range are hopeful to provide new insights of the microscopic model for thermodynamic properties in vitreous systems. Future experiments with improved background scattering in the low energy range could possibly reveal better correlation between phonon density of states and thermal expansion.

ACKNOWLEDGMENTS

The authors are grateful to P. Salmon and A. Zeidler for stimulating discussion. We also thank G. Moore for discussion on the Raman scattering results on a similar study. This research used resources at the Spallation Neutron Source, a DOE Office of Science User Facility operated by the Oak Ridge National Laboratory.

[1] U. Buchenau, N. Nucker, and A. J. Dianoux, Phys. Rev. Lett. **53**, 2316 (1984).
[2] T. S. Grigera, V. Martin-Mayor, G. Parisi, and P. Verrochio, Nature (London) **422**, 289 (2003).
[3] N. Xu, M. Wyart, A. J. Liu, and S. R. Nagel, Phys. Rev. Lett **98**, 175502 (2007).
[4] S. Caponi, S. Corezzi, D. Fioretto, A. Fontana, G. Monaco, and F. Rossi, Phys. Rev. Lett. **102**, 027402 (2009).
[5] A. Monaco, A. I. Chumakov, Y.-Z. Yue, G. Monaco, L. Comez, D. Fioretto, W. A. Crichton, and R. Rüffer, Phys. Rev. Lett. **96**, 205502 (2006).
[6] A. I. Chumakov, G. Monaco, A. Monaco, W. A. Crichton, A. Bosak, R. Rüffer, A. Meyer, F. Kargl, L. Comez, D. Fioretto, H. Giefers, S. Roitsch, G. Wortmann, M. H. Manghnani, A. Hushur, Q. Williams, J. Balogh, K. Parlinski, P. Jochym, and P. Piekarz, Phy. Rev. Lett. **106**, 225501 (2011).
[7] A. I. Chumakov, G. Monaco, A. Fontana, A. Bosak, R. P. Hermann, D. Bessas, B. Wehinger, W. A. Crichton, M. Krisch, R. Rüffer, G. Baldi, G. Carini, Jr., G. Carini, G. D'Angelo, E. Gilioli, G. Tripodo, M. Zanatta, B. Winkler, V. Milman, K. Refson, M. T. Dove, N. Dubrovinskaia, L. Dubrovinsky, R. Keding, and Y. Z. Yue, Phys. Rev. Lett. **112**, 025502 (2014).
[8] A. Monaco, A. I. Chumakov, G. Monaco, W. A. Crichton, A. Meyer, L. Comez, D. Fioretto, J. Korecki, and R. Rüffer, Phys. Rev. Lett. **97**, 135501 (2006).
[9] G. Baldi, A. Fontana, G. Monaco, L. Orsingher, S. Rols, F. Rossi, and B. Ruta, Phys. Rev. Lett. **102**, 195502 (2009).
[10] B. Ruffle, S. Ayrinhac, E. Courtens, R. Vacher, M. Foret, A. Wischnewski, and U. Buchenau, Phys. Rev. Lett. **104**, 067402 (2010).
[11] Amorphous Solids Low Temperature Properties, edited by W. A. Phillips (Springer Verlag, Berlin, 1981).
[12] Q. Mei, C. J. Benmore, S. Sen, R. Sharma, and J. L. Yarger, Phys. Rev. B **78**, 144204 (2008).
[13] M. Sitarz, W. Mozgawa, and M. Handke, J. Mol. Struc. **511-512**, 281 (1999).
[14] P. Tandon and H. Boek, J. Non-Cryst. Solids **317**, 275 (2003).
[15] See Supplemental Material at http://link.aps.org/supplemental/10.1103/PhysRevB.97.054311 for experimental details.
[16] F. L. Galeener, A. J. Leadbetter, and M. W. Stringfellow, Phys. Rev. B **27**, 1052 (1983).
[17] E. Fabiani, A. Fontana, and U. Buchenau, J. Chem. Phys. **128**, 244507 (2008).
[18] S. N. Taraskin and S. R. Elliott, Phys. Rev. B **55**, 117 (1997).
[19] D. L. Price and J. M. Carpenter, J. Non-Cryst. Solids **92**, 153 (1987).
[20] P. N. Sen and M. F. Thorpe, Phys. Rev. B **15**, 4030 (1977).
[21] R. J. Bell, N. F. Bird, and P. Dean, J. Phys. C **1**, 299 (1968).
[22] D. S. Knight, C. G. Pantano, and W. B. White, Mat. Lett. **8**, 156 (1989).
[23] G. Scannell, A. Koike, and L. Huang, J. Non-Cryst. Solids **447**, 238 (2016).
[24] G. S. Henderson and M. E. Fleet, Can. Mine. **33**, 399 (1995).
[25] R. Haworth, G. Mountjoy, M. Corno, P. Ugliengo, and R. J. Newport, Phys. Rev. B **81**, 060301 (2010).
[26] P. W. Anderson, B. I. Halperin, and C. M. Varma, Phil. Mag. **25**, 1 (1972).
[27] A. J. Leadbetter, Phys. Chem. Glasses **9**, 1 (1968).
[28] W. M. MacDonald, A. C. Anderson, and J. Schroeder, Phys. Rev. B **31**, 1090 (1985).
[29] M. A. Ramos and U. Buchenau, Phys. Rev. B **55**, 5749 (1997).
[30] R. C. Zeller and R. O. Pohl, Phys. Rev. B **4**, 2029 (1971).
[31] G. White, J. Phys. D: Appl. Phys. **6**, 2070 (1973).
[32] B. Ruta, G. Baldi, V. M. Giordano, L. Orsingher, S. Rols, F. Scarponi, and G. Monaco, J. Chem. Phys. **133**, 041101 (2010).
[33] P. C. Shultz, J. Am. Ceram. Soc. **59**, 214 (1976).
[34] H. Shermer, J. Res. Natl. Bur. Stand. **57**, 97 (1956).
[35] Z. K. Liu, Y. Wang, and S. Shang, Sci. Rep. **4**, 7043 (2014).
[36] G. Ernst, C. Broholm, G. Kowach, and A. Ramiraz, Nature (London) **396**, 147 (1998).